ELSEVIER

Polymer 44 (2003) 2117–2128

polymer

www.elsevier.com/locate/polymer

Self-assembly of amphiphilic di and triblock copolymers of styrene and quaternized 5-(*N*,*N*-diethylamino) isoprene in selective solvents

Izabel C. Riegel[a,b,*], Dimitrios Samios[a], Cesar L. Petzhold[a], Adi Eisenberg[b]

[a]*Instituto de Química, Universidade Federal do Rio Grande do Sul, Av. Bento Gonçalves, 9500, CP 15003, Porto Alegre RS 91501-970, Brazil*
[b]*Department of Chemistry, McGill University, 801 Sherbrooke Street West, Montreal, Que., Canada H3A 2K6*

Received 14 June 2002; received in revised form 18 December 2002; accepted 20 December 2002

Abstract

Self-association of highly asymmetric block copolymers of styrene and quaternized 5-(*N*,*N*-diethylamino)isoprene was studied. After quaternization with dimethyl sulfate, the di and triblock copolymers consisted of a long block of polystyrene (PS) with a short poly[5-(*N*,*N*,*N*-diethylmethylammonium)isoprene][methyl sulfate](PAI) block at one or both chain ends, respectively. The aggregates were prepared by first dissolving the copolymers in an organic solvent and then adding water to induce the segregation of the PS chains. Pure DMF, THF or dioxane was used as the organic solvent, as well as DMF/THF mixtures. The critical water content (cwc) and the morphologies were studied as a function of the common solvent, initial copolymer concentration and architecture (di or triblock) by static light scattering and by Transmission Electron Microscopy (TEM), respectively. It was found that both, the cwc and the morphologies of the aggregates are most strongly affected by the nature of the common solvent. Some unexpected behaviors were found for the triblock copolymer. Morphologies of a triblock copolymer in various mixtures of DMF and THF, quenched at determined water contents, were investigated in order to study the degree of morphological control that can be achieved solely as function of the organic solvent composition. Multiple morphologies have been found including equilibrium morphologies and kinetically trapped ones. Finally, the stability of primary micelles prepared in DMF was studied by DLS, upon dilution with DMF and water, and a possible mechanism for the destabilization of the aggregates is proposed.
© 2003 Elsevier Science Ltd. All rights reserved.

Keywords: Nanoaggregates; Microscopy; Cationic polyelectrolyte

1. Introduction

Amphiphilic molecules can self-assemble in selective solvents into a variety of microstructures. Compared to small molecular weight molecules, aggregates from block copolymer amphiphiles are thermodynamically and kinetically more stable, broadening their potential applications. Self-assembly of amphiphilic block copolymers has long been investigated. Many groups, including the groups of Eisenberg [1,2], Kabanov [3,4], Discher and Hammer [5,6], Antonietti [7,8], Müller [9,10], Maskos [11,12], Liu [13,14], Winnik [15], among others, are active in the field. When the hydrophobic block is in the core and the hydrophilic block is in the corona, the aggregates form regular micelles and the opposite is true for inverse micelles, i.e. the hydrophilic block forms the core and the hydrophobic the corona. Due to their very interesting particular properties, block copolymer micellar systems hold great promise in areas such as biology, colloid science, and encapsulation technology [16,17] among others [18,19].

Crew-cut like structures consist of a class of aggregates made from amphiphilic block copolymers in highly polar media, in which the core-forming block is much longer than the corona one [20]. Because of the relative composition of the blocks, the aggregates are prepared by an indirect method; the copolymer is first dissolved in a good solvent for both blocks and then water is added as a precipitant to induce the segregation of the hydrophobic blocks. As opposed to star-micelles [21], where the longer corona-forming blocks induce the formation of spherical micelles, it was found that crew-cut aggregates can give rise to several morphologies, as for example spheres, rods and vesicles [22].

---

* Corresponding author. Address: Instituto de Química, Universidade Federal do Rio Grande do Sul, Av. Bento Gonçalves, 9500, CP 15003, Porto Alegre, RS 91501-970, Brazil. Tel.: +55-51-33166291; fax: +55-51-33167304.

E-mail address: iriegel@bravo436.chem.mcgill.ca (I.C. Riegel).

0032-3861/03/$ - see front matter © 2003 Elsevier Science Ltd. All rights reserved.
doi:10.1016/S0032-3861(03)00013-2

Crew-cut micelle-like aggregates of highly asymmetric copolymers of polystyrene-*b*-poly (acrylic acid) diblock copolymers (PS-*b*-PAA), which in aqueous solution form anionic micelles, have been extensively studied by Eisenberg et al. Since 1995 [2], it was identified a vast array of structures [23] and a detailed investigation have begun on the thermodynamic and kinetic aspects that induce morphogenesis [24–26]. Many factors were found to influence the resulting morphologies, as for example, the copolymer composition and concentration [27], the nature of the common solvent [28], the type and concentration of added ions [29], among other factors [30].

Cationic aggregates have not been investigated as much as the anionic ones. Regarding biological interests, cationic aggregates have shown to be promising in their possible applications [31,32]. Polymers are known to modify the interfacial properties of the surfaces they adsorb on [33,34]. For instance, many interfacial processes of interest involve microorganisms and the surface properties of bacterial cells have an impact on their properties. Therefore, the electrostatic forces acting on amphiphilic copolymer aggregates, combined with the various controlled morphologies that can be obtained from these materials, can be used to systematically tune the chemical and surface charge properties of many living cells. Very recently, Cameron et al. [35,36] have reported the self-assembly of a new cationic amphiphilic block copolymer, polystyrene-*b*-poly(*N*,*N*,*N*-trimethylammoniumethylene acrylamide chloride (PS-*b*-PTMEACl) which has shown potential application as bile-salt sequestrant (BBS). Moreover, in the case of wastewater treatment, cationic polyelectrolytes have been reported to play an important role.

5-(*N*,*N*-Dialkylamino)isoprenes (AI) are excellent monomers for synthesis of ionic polymers, since they can be anionically polymerized and by quaternization of tertiary amino group, positively charged polyelectrolytes can be obtained [37]. The homopolymerization of these monomers has been investigated as well as the structure and properties of the resulting homopolymers [38]. Moreover, the copolymerization of the AI monomers with a non-polar monomer (styrene) have been described [39], and the solution properties of the non-quaternized amphiphilic block copolymers of PAI and PS have been investigated in various solvents [40]. Also, the solution and bulk properties of triblock copolyampholytes from 5-[*N*,*N*-dimethylamino] isoprene, styrene and methacrylic acid have been investigated [41].

In this work, cationic polyelectrolytes were obtained by the anionic copolymerization of 5-(*N*,*N*-diethylamino)isoprene and styrene (PAI-*b*-PS and PAI-*b*-PS-*b*-PAI) and subsequent quaternization of the tertiary amino group present on the poly(aminoisoprene) block(s). The positively charged block(s) are expected to be fully ionized and therefore, not subjected to pH change effects. Because of their composition, of ca. 90 mol% of polystyrene, the quaternized di and triblock copolymers are not directly soluble in water. Therefore, the above-mentioned indirect method of preparation of the micellar aqueous solutions is required; all the obtained structures could be classified as crew-cut aggregates.

The scope of the present paper is to first present a general characterization of cationic micelles from PAI-*b*-PS and PAI-*b*-PS-*b*-PAI, regarding the main aspects of their micellization behavior and resulting morphologies. It is worth mentioning that comparing to the previously reported PS-*b*-PAA systems, the presently studied copolymers differ in some ways. The PS-*b*-PAA copolymers are ionizable molecules (anionic) whereas the PAI-*b*-PS and PAI-*b*-PS-*b*-PAI bear permanent charges (cationic). In addition, here we have investigated the role of the architecture (tri versus diblock) on the self-assembly of amphiphilic block copolymers, which has not been studied previously for the PS-PAA systems. The investigations were carried out following some procedures previously described for the PAA-*b*-PS copolymers. As a consequence, whenever suitable, we discuss the similarities and dissimilarities between these two systems involving their aggregation aspects and resulting morphologies.

Initially, we describe the microphase separation of solutions of di and triblock copolymers in various solvents due to the addition of water. The aggregation behavior was characterized by static light scattering (SLS) in various solvents: *N*,*N*-dimethylformamide (DMF), dioxane and tetrahydrofuran (THF). This technique allows the determination of the critical water content (cwc) at which phase separation starts, since the scattered static light intensity depends on the particles sizes or the number of particles in solution. The dependence of the final morphology with the copolymer concentration, nature and composition of the organic solvent is investigated further. Afterwards, mixing solvents were employed in order to investigate the morphological control that can be achieved for the same copolymer, exclusively as a function of the solvent composition. Finally, the stability of primary spherical micelles in solution was investigated by DLS.

A parallel study of the micellization kinetics of these crew-cut aggregates in dioxane/water mixtures, has been conducted using the turbidity method [42], and will be soon reported in a forthcoming paper [43].

2. Experimental section

2.1. Block copolymers synthesis and quaternization

The triblock copolymers were obtained via sequential anionic polymerization of 5-(*N*,*N*-diethylamino)isoprene followed by styrene and again by 5-(*N*,*N*-diethylamino)isoprene. The diblocks were obtained by withdrawing an aliquot from the reactor before the second addition of the aminoisoprene type monomer. A description of the synthesis procedure can be found elsewhere [44]. Size exclusion chromatography (SEC) was used to determine the degree of polymerization and the polydispersity of the copolymers, on a Waters Instrument, equipped with a differential refractometer detector and PS/DVB columns (Waters Styragel). The copolymers composition was determined by ^{1}H NMR. The spectra were recorded on a Varian VXR 200 Hz spectrometer in deuterated chloroform at 20 °C. The calculus of the degree of polymerization of the polystyrene relative to the poly[5-(*N*,*N*-diethylamino) isoprene] was performed according to what was previously described [39].

Two sets of copolymers with different molecular weights but with approximately the same composition were investigated. The relevant data for the materials are summarized in Table 1.

After synthesis, the copolymers were quaternized with dimethyl sulfate, in a mixture of solvents (methanol/benzene), according to a method already described in the literature [37], in order to obtain positively charged blocks at one or both chain ends, respectively. The quaternized di and triblock species are designated as polystyrene-*b*-poly[5-(*N*,*N*,*N*-diethylmethylammonium)isoprene][methyl sulfate] (PS-*b*-PAI) and poly[5-(*N*,*N*,*N*-diethylmethylammonium) isoprene][methyl sulfate]-*b*-polystyrene-*b*-poly[5-(*N*,*N*,*N*-diethylmethylammonium)isoprene][methyl sulfate] (PAI-*b*-PS-*b*-PAI).

2.2. Self-assembly procedure and quenching method

The copolymers were first dissolved in the organic solvent (DMF, THF, dioxane or mixtures of DMF/THF) to desired concentrations, and allowed to stir overnight at room temperature. After that, deionized water was added at a rate of 0.5 wt% per minute, until pre-determined contents. At very low concentrations of water, isolated chains are dispersed in the solution. As the addition of water progresses, the quality of the solvent for the longer block (polystyrene) gradually decreases and the aggregates are formed at a cwc. DMF/THF mixtures were used in different compositions (from 5/95 to 70/30 wt%), in order to investigate the changes in the morphologies as a response to the nature of the organic solvent. Solutions (1 wt%) were prepared by the solubilization of the copolymer PAI_{11}-*b*-PS_{228}-*b*-PAI_{11} in DMF/THF mixtures. Deionized water was, then, added at a rate of 0.5 wt% every 1 min, upon vigorous stirring, until pre-determined water contents (from 5 to 50 wt%). After that, a large amount of water was added to the solution in order to quench the resulting morphology. We assume, at this point, that the structure is frozen, in a process similar to freeze the structures formed in bulk of some copolymers systems, which are annealed at high temperature by dropping the temperature. The solution was then dialyzed against water for 3 days to remove the organic solvents. The colloidal solutions preparation will be given in more details in the following sections, according to each experimental technique.

Table 1
Molecular characteristics of block copolymers of styrene and 5-(*N*,*N*-diethylamino)isoprene

Copolymer[a]	PAI content[b] (mol%)	M_n (g/mol)[c]	M_w/M_n[c]
PAI_{11}-*b*-PS_{228}-*b*-PAI_{11}	8.8	26,800	1.2
PAI_{11}-*b*-PS_{228}	4.4	20,900	1.4
PAI_6-*b*-PS_{120}-*b*-PAI_5	8.3	13,900	1.2
PAI_6-*b*-PS_{120}	4.9	13,600	1.2

[a] The numbers indicate the number average degrees of polymerization of each block.

[b] The PAI content was determined by NMR relative to that of the PS block.

[c] Parameters determined by SEC.

2.3. Light scattering measurements

Static and dynamic light scattering measurements (SLS and DLS) were performed at 20 °C on an automatic BI-200M goniometer and a BI-9000 AT digital correlator (Brookhaven Instruments). A Spectra Physics (model 127) He–Ne laser ($\lambda = 632.8$ nm) was used as light source. Intensity time correlation functions were obtained in multiple-τ mode in the angular range from 45° to 145°.

2.3.1. Static light scattering measurements

The polymer/solvent solutions were prepared as described in Section 2.2. The solutions were filtered through a Millipore filter of nominal pore size of 0.45 μm into dust-free quartz scintillation vials. Milli-Q water was previously filtered through a 0.2 μm pore size and added to the polymer solutions (0.5 wt% per minute). The scattered light intensity corresponding to each water concentration (from 0 wt% up to ca. 30 wt%) was recorded 15 min after each water jump and mixing of the solution. The scattered light intensity was collected at 90°.

2.3.2. Dynamic light scattering

The triblock copolymer PAI-*b*-PS-*b*-PAI ($M_w = 26{,}800$ g/mol) was first dissolved in DMF at a concentration of 1 wt% and subsequently deionized water was added until 30 wt%. Both the solution and the water were filtered through suitable Millipore filters of pore sizes of 0.45 and 0.22 μm, respectively. The resulting stock solution was obtained through dialysis of the polymer/DMF/water solution, and was systematically diluted with DMF, in a first set of DLS experiments, and with water, in another set of DLS experiments. The intensity time correlation functions were recorded for each resulting solution, at various angles, and the evaluation of the hydrodynamic radius was obtained using the CONTIN algorithm.

2.4. Transmission electron microscopy

The experiments were carried out on a JEM2000-FX microscope operating at 80 kV. Aqueous aggregate solutions free of organic solvents were used to prepare the TEM samples. A drop of the dilute solution (10–20 times dilution) was placed onto copper grids pre-coated with Formvar and carbon and let evaporate at room temperature.

3. Results and discussion

3.1. Aggregation behavior in various solvents

The indirect method of preparation of the crew-cut micelles requires first the dissolution of the copolymer in an organic solvent that is good for both blocks. DMF, THF and 1,4-dioxane were tentatively used as good solvents for both PS and PAI. Although these three solvents are considered good for the PS block, on trying to dissolve the PAI homopolymer on the three solvents, only THF was able to solubilize the homo-PAI, whereas DMF and dioxane were not. Besides, studies presently carried in our lab [40] revealed that, solutions of the triblock copolymer PAI-*b*-PS-*b*-PAI in THF showed no angular dependence of the static light scattered intensity, according to the Zimm method. On the contrary, when DMF or dioxane was used as the solvent, a strong angular dependence of the static light scattered intensity were observed. In spite of that, since both DMF and dioxane are able to solubilize the copolymers into macroscopically homogeneous solutions, under a practical point of view, all the three solvents were assumed to be good for both blocks.

On the self-assembly of amphiphilic block copolymers, as water is added to the initial solution, the quality of the solvent decreases for the hydrophobic block. When the water content reaches a critical value, defined as cwc, the hydrophobic segments associate to form micelles and the solution undergoes microphase separation. The driving force for the micellization is the existence of attractive forces between the amphiphiles and repulsive forces that prevent the infinite growth of the aggregate.

The initial copolymer concentration in various solvents (DMF, THF and dioxane), before the addition of water, ranged from 10^{-5} to 10^{-2} g/g. The static scattered light intensity as a function of the water content can be seen in Fig. 1, corresponding to solutions of PAI_{11}-*b*-PS_{228} and PAI_{11}-*b*-PS_{228}-*b*-PAI_{11}, initially at 0.1 wt%, in various solvents. At relatively low water concentrations, the static scattered light intensity changes little. When the water content reaches a certain value, the scattered light increases abruptly, indicating the attainment of a water content that corresponds to the cwc. At the cwc, the diblock solutions became cloudy, irrespective of the initial copolymer concentration and solvent nature. On the other hand, the triblock copolymer solutions did not become cloudy when the initial solvent was DMF. In those cases, the increase in the scattered light intensity at cwc is not too steep. Even beyond the cwc, the SLS intensity increases slowly with further addition of water. These triblock solutions did not turn cloudy at water contents up to ca. 50 wt%. This phenomenon will be better understood in Section 3.2 when we will discuss the resulting morphologies in each solvent.

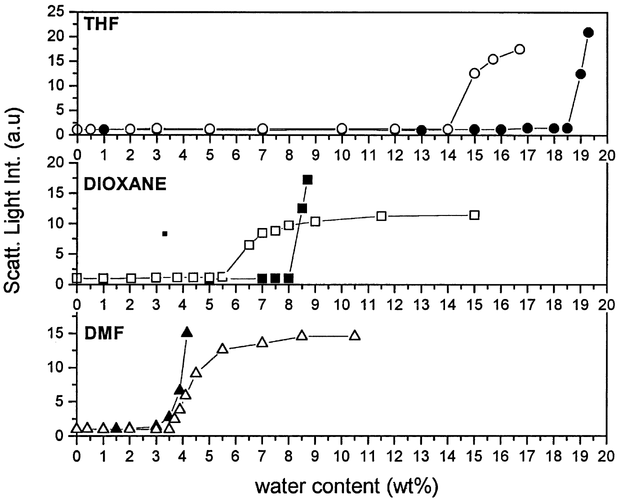

Fig. 1. Scattered light intensity as a function of water content (wt%) for PAI_{11}-*b*-PS_{228} (closed symbols) and PAI_{11}-*b*-PS_{228}-*b*-PAI_{11} (open symbols) in various solvents. The initial copolymer concentration corresponds to 0.1 wt%.

It can also be seen in Fig. 1 that, due to different interactions between the solvent and the copolymer forming blocks, the cwc shifts to higher values as the common solvent changes from DMF to dioxane and then to THF. Since PS is a non-polar polymer, its interaction with the solvents can be predicted from some parameters, named the solubility parameter δ and the dielectric constant ε. These two parameters are related to the parameter χ, which reflects the strength of the interaction between the polymer and the solvent. According to what was discussed in a previous paper [28], the polystyrene–solvent interaction should be stronger in THF, followed by dioxane and DMF, since the solubility parameter of the THF is the closer to that of homo-PS when compared to dioxane and DMF. Although the parameter χ is not available for the quaternized homopoly(aminoisoprene); homo-PAI; it is known that it is not soluble in dioxane nor in DMF, but it is soluble in THF. Therefore, within this simple approach it was expected that the solubility of the copolymers would be higher in THF, than in dioxane or DMF.

Regarding the effect of the initial copolymer concentration on the cwc, it was observed that the cwc shifts to higher values as the initial copolymer concentration decreases (Fig. 2). This behavior reflects the higher solubility of the copolymer in the water/solvent mixtures at lower concentrations. Fig. 2 shows a linear relationship between the cwc and the logarithm of the copolymer initial concentration for both di and triblock copolymers. Also, the slopes of the straight lines differ according to the solvent, being higher when the solvent is THF; smaller when the solvent is dioxane and smallest when it is DMF, which is a

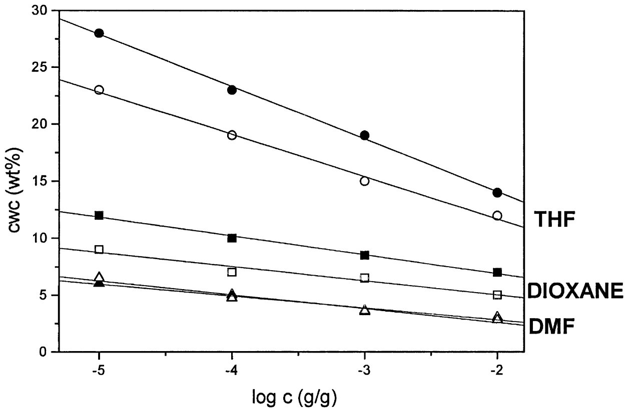

Fig. 2. Critical water concentration (cwc) as a function of the copolymer concentration for the diblock PAI_{11}-*b*-PS_{228} (closed symbols) and the triblock PAI_{11}-*b*-PS_{228}-*b*-PAI_{11} (open symbols) copolymers solutions in various solvents: THF (circles), dioxane (squares) and DMF (up triangles).

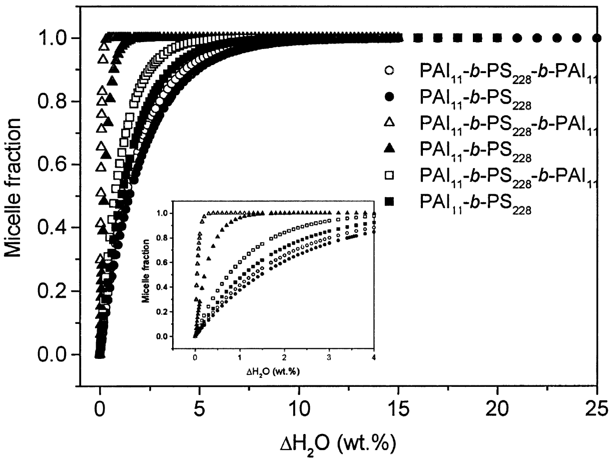

Fig. 3. Micelle fraction as a function of water increment for the diblock and the triblock copolymers solutions in various solvents: THF (circles), dioxane (squares) and DMF (up triangles). The insert shows the micelle fraction behavior in the first stages of micellization (ΔH_2O varying from 0 to 4 wt%).

reflection of the different interactions between the copolymer blocks and the organic solvent.

Considering the copolymer architecture, when the organic solvent is DMF, the cwc of the di and of the triblock copolymer are very close, considering the same initial concentration. The differences between the cwc become higher when the organic solvent is changed to dioxane and then to THF. It can be seen in Fig. 2 that the diblock copolymer is more soluble in the solvent/water mixtures than the triblock, as reflected by the smaller cwc values of the latter one. This behavior is yet not clear, since it would be expected that the extra charged aminoisoprene block, present in the triblock copolymer, when compared to the diblock, would improve the triblock solubility in water. In regard to this, we proposed, in a recent study where we describe a new morphology found for this triblock copolymer, that, probably, the extra aminoisoprene block is responsible for a physical crosslinking, which would increase the viscosity of the solution and lower the cwc [44].

In the course of water addition beyond the cwc, the copolymer single-chains continuously associate to form more and more micelles in solution; therefore, the concentration of unassociated molecules decrease down to essentially zero. Fig. 3 shows a plot of the micelle fraction against the increment of the water content in various solvents, with the insert showing the early stages of the micellization (ΔH_2O from 0 to 4 wt%). The micelle fraction is defined as the ratio of the concentration of associated polymer, i.e. the difference between the initial copolymer concentration and critical micellization concentration; to the total concentration of polymer. The increment of the water content, ΔH_2O; stands for the content of water beyond the cwc. The equations that relate the micelle fraction and the increment of water were derived and extensively discussed in previous papers for PS-*b*-PAA of various compositions [45]. As demonstrated, the micelle fraction increases exponentially with the increment of water in a way that is directly dependent on the nature of the organic solvent [28].

It is clear from Fig. 3 that different solvents lead to micelle formation in different regions of water contents. In THF, both di and triblock copolymers undergo micellization over a broader range of water content than in dioxane or DMF. In DMF, the micelle fraction shows the strongest dependence on the water increment. In this solvent, the micellization process will be virtually completed within 0.5 wt% of water increment for the triblock copolymer.

When compared to THF, a much higher water increment, 24 wt%, is required to reach the same degree of micellization. The copolymer microstructure also influences the dependence of the micelle fraction on the water increment. For example, a diblock copolymer solution in THF will require 3.5 wt% of water beyond the cwc to reach 80% of micellization; on the other hand, 3 wt% is needed to attain the same degree of micellization for a triblock copolymer solution in the same solvent. The influence of the architecture on the micelle fraction at each water increment becomes more pronounced as we go from DMF, then to dioxane and finally to THF.

Since the relationship between the micelle fraction and the increment of the water content is exponential, mostly of the micellization process takes place at relatively low water increments. Generalizing the copolymers behavior in all solvents, 80% of micellization will be attained in the range of 0.5–3.5 wt%; the remaining 20% of micellization will take place over an increment of 3.6–26 wt% of water, depending on the solvent.

3.2. Morphologies from pure solvents

Morphologies of crew-cut aggregates from copolymers of styrene and quaternized 5-(*N*,*N*-diethylamino)isoprene were studied as a function of the organic solvent, initial concentration and copolymer molecular weight and architecture. The aggregates could be directly observed by TEM due to the high T_g of polystyrene and their dimensions were measured readily from the micrographs. It was found that the investigated di and triblock copolymers yielded multiple morphologies in various solvents (Table 2).

In the early stages of aggregation, a thermodynamic equilibrium between unimers and aggregates can be assumed. As more water is added, the organic solvent is progressively extracted from the cores up to a point where the aggregates can be considered kinetically frozen. In the course of the micellization phenomena, many different morphologies can result. If one or another morphology will be found, it will be a function of a delicate force balance of mainly three components of the free energy of micellization; that is the stretching of the core-forming blocks, the repulsion among the corona chains and the interfacial energy between the core and the outside solvent. The above-mentioned force balance will be influenced by the copolymer concentration, nature of the common solvent, the relative block lengths and other factors [46].

It has been reported that the nature of the organic solvent is one of the most important morphogenic factors, since polymer–solvent interactions determines the coil dimensions of each block. Moreover, the role of the solvent is very important on the aggregation since it has an impact on the free energy of micellization [47,48]. In THF, for example, PS chains are more extended, since the PS–solvent interaction is stronger when compared to dioxane or DMF. Therefore, when the solvent is THF, it is expected that the dimensions of the aggregate would be bigger because the solvent content in the core will be higher [28]. The way the PS-*b*-PAI and PAI-*b*-PS-*b*-PAI copolymers are expected to assemble, will be a direct consequence of the degree of swollenness of mainly the hydrophobic chains, since ca. of 90 mol% of the copolymer is composed by PS (see Table 1).

One of the most interesting finding on the present copolymer systems was the formation of an unexpected morphology, resembling the shape of a bowl. The bowl-shaped aggregates consist of a new morphology encountered only in the triblock copolymers in dioxane and THF. This novel morphology was extensively described and a possible mechanism of formation was proposed in a recent paper [44].

Fig. 4 shows TEM micrographs demonstrating the morphologies obtained from PAI_{11}-*b*-PS_{228} and PAI_{11}-*b*-PS_{228}-*b*-PAI_{11} at initial concentration of 1 wt% in various solvents. It can first be observed that the copolymer architecture plays a role on the resulting morphology. Comparing Fig. 4A and D, primary micelles are seen to coexist with some short rods in the case of the diblock whereas in the triblock copolymer, mainly spherical aggregates are observed in DMF as the common solvent. In both cases, the average diameter of the primary micelles is 23 ± 3 nm, which indicates that the diblock copolymer showed a shift on the morphology boundary [22] when compared to the triblock. The formation of mainly spherical aggregates in DMF, can be attributed to the high dielectric constant ($\varepsilon = 38.2$) of this solvent, which decreases the PS-solvent interaction. In DMF, the repulsion among the corona chains is high and consequently the degree of stretching of the PS chains is decreased, leading to the formation of this type of aggregates. These results are in agreement with what was observed for the PS-*b*-PAA copolymer with various PAA contents [45,46]. What is curious, though, is the fact both di and triblock copolymers have yielded spherical aggregates with the same average diameter. We would expect that the average size of the spherical aggregates from the triblock would be lower than the size of the aggregates from the diblock copolymer, since the triblock has hydrophilic blocks at both PS chain ends. The degree of stretching (S_c) of the PS blocks, which is expressed as the ratio of the micelle radius to the end-to-end distance in the unperturbed state (R_0), has been discussed for the PAA-*b*-PS copolymers in a previous paper [49,50]. For the present PAI and PS copolymers, the S_c theoretically would result the same for both copolymers, since di and triblocks have the same PS block length. So, in the case of the triblock, we suggest that, instead of taking the PS degree of

Table 2
Morphologies of PAI_{11}-*b*-PS_{228}-*b*-PAI_{11} and PAI_{11}-*b*-PS_{228} in different solvents. (S = spheres; R = rods; L = lamellae; V = vesicles; BS = bowl-shapes; CM compound micelles)

	Concentration (g/g)		
	10^{-4}	10^{-3}	10^{-2}
DMF			
Diblock	S	S	S + R
Triblock	S	S	S
Dioxane			
Diblock	Interconnected V (<250 nm)	Interconnected CM (<250 nm)	CM (up to 500 nm)
Triblock	CM (<250 nm)	BS + CM	BS
THF			
Diblock	S + R + L	S + R + V	V
Triblock	S + R + BS	R + BS	BS

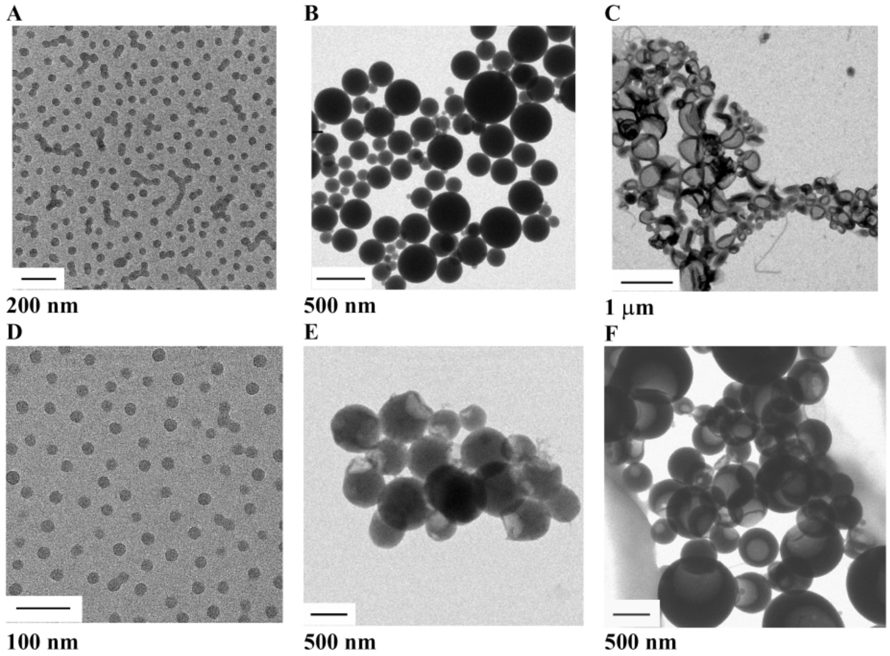

Fig. 4. TEM micrographs of crew-cut aggregates from PAI$_{11}$-*b*-PS$_{228}$ (first row) and PAI$_{11}$-*b*-PS$_{228}$-*b*-PAI$_{11}$ (second row) at 1 wt% initial concentration in various solvents: DMF (first column); dioxane (second column) and THF (third column).

polymerization, it is more suitable to take half of this value to calculate R_0. Therefore, the S_c results 1.6 for the triblock and 1.2 for the diblock copolymer.

In a recent paper, micelle sizes of di and triblock copolymers of poly(oxyethylene) and poly(oxybutylene) were investigated by light scattering experiments. Both copolymers have shown the same micellar size by due to a folding of the core blocks [51].

When dioxane is employed as the common solvent, the morphology change is more evident when comparing the di and triblock copolymer. Fig. 4B shows compound micelles from PAI$_{11}$-*b*-PS$_{228}$ in dioxane (1 wt% initial concentration) and Fig. 4E shows bowl-shaped morphologies from PAI$_{11}$-*b*-PS$_{228}$-*b*-PAI$_{11}$ in the same solvent and same initial concentration. It was suggested in a previous paper [44] that compound micelles and bowl-shapes are somehow related regarding their mechanism of formation. Both compound micelles and bowl-shapes are believed to be composed of an assembly of reverse micelles.

On changing to THF as the common solvent, the diblock (Fig. 4C) and the triblock (Fig. 4F) formed vesicles and bowl-shaped morphologies, respectively, at 1 wt%. Among the three used organic solvents, THF happened to be the most interesting in terms of the variety of morphologies possible to be obtained. Table 2 shows that spheres, rods, lamella, vesicles and a new morphology, the bowl-shape, were encountered over the range of initial concentration used.

Despite keeping the composition approximately constant, the lower molecular weight set of copolymers; PAI$_{6}$-*b*-PS$_{120}$-*b*-PAI$_{5}$ and PAI$_{6}$-*b*-PS$_{120}$, yielded mostly compound micelles. It is known that the total block length is also an important morphogenic factor [27]. The low molecular weight of the copolymers also lowers the bending modulus, in a way similar to what happens on the micellization of surfactants [52]. Vesicles formation is, therefore, not favored because the tendency to form closed bilayer structures (precursors of vesicles) highly decreases as the bending modulus decreases. Besides compound micelles, bowl-shaped (BS) aggregates were found from the triblock copolymer PAI$_{6}$-*b*-PS$_{120}$-*b*-PAI$_{5}$ in dioxane, at initial concentration of 1 wt%. These experimental results may indicate that the precursor for the BS morphology is not bilayer structures, but, most probably, compound micelles, confirming what we have already speculated [44].

Compound micelles and large compound micelles were mostly encountered for PAI$_{11}$-*b*-PS$_{228}$-*b*-PAI$_{11}$ and PAI$_{11}$-*b*-PS$_{228}$ in dioxane and for PAI$_{6}$-*b*-PS$_{120}$-*b*-PAI$_{5}$ and PAI$_{6}$-*b*-PS$_{120}$ in all solvents and all concentrations. As we have already mentioned, this morphology constitutes an assembly of reverse micelles, immersed in a continuous PS phase, surrounded by the hydrophilic blocks. LCMs were first reported in 1996 [50] and it was found to result from diblock copolymers of very short hydrophilic blocks (PS$_{200}$-*b*-PAA$_{4}$ in DMF). The most typical characteristics of the LCMs are their high polydispersity and very large sizes (sometimes up to 1 μm). A possible explanation for these peculiar features of LCMs, can be given based on the work conducted by Esselink et al. [53]. They have studied the process of reaching the equilibrium micellar size and structure of reverse micelles and reported that the larger the micelle equilibrium size, the broader the size distribution than can be expected. The frequent occurrence of LCM in the present studied copolymers is yet not clear, since their corona-forming blocks are not considered very short. Perhaps, the formation of LCMs is most strongly related to the hydrophilic block–organic solvent interactions and the copolymer molecular weight than to the relative hydrophobic/hydrophilic block lengths.

3.3. Morphologies as a function of solvent composition and water content

It was presented in Section 3.2 that the same copolymer can yield different morphologies, depending on the solvent and initial composition. Between these two morphogenic factors, the nature of the common solvent most strongly affects the resulting morphology, according to what can be seen in Table 2. Mostly primary micelles were obtained in DMF and a broad range of morphologies was found in THF. Since the interactions between the solvent and the hydrophobic/hydrophilic blocks are very determinant on the self-assembly process, mixing solvents is expected to make possible the formation of a much broader range of morphologies, when compared to pure solvents.

Structures formed from the copolymer PAI_{11}-*b*-PS_{228}-*b*-PAI_{11} in mixtures of THF and DMF, in different compositions, were studied. Besides the solvent composition effect, we also explored the role of the water content on the morphologies, keeping the initial copolymer concentration always at 1 wt%. After the solubilization step and water addition, the resulting aggregates were trapped at determined water contents, by adding a large amount of water to the solution.

The cwc was followed as a function of the solvent composition (Fig. 5). As expected, the cwc decreases as the DMF content increases, since in pure DMF the cwc is lower than in pure THF. However, the relationship between the cwc and the DMF content cannot be described through a linear combination.

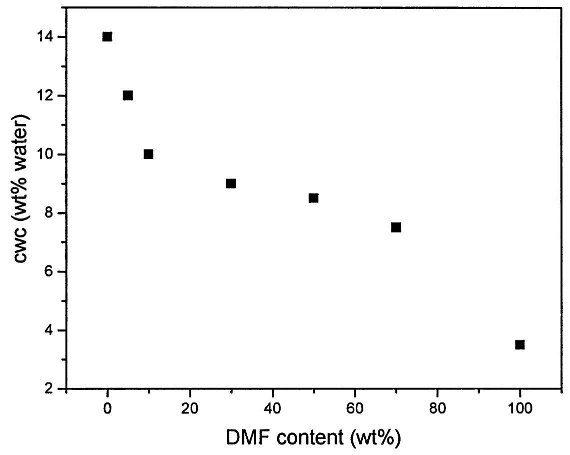

Fig. 5. Cwc as a function of the solvent composition for solutions of PAI_{11}-*b*-PS_{228}-*b*-PAI_{11} initially at 1 wt%.

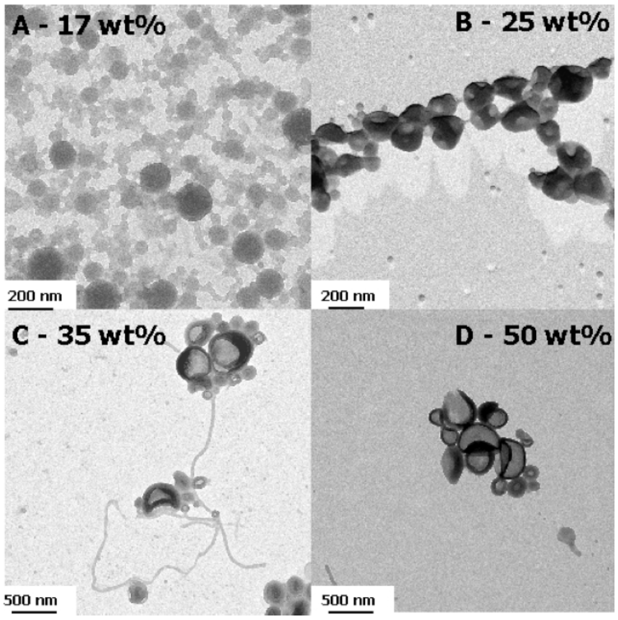

Fig. 6. TEM images of morphologies obtained from PAI_{11}-*b*-PS_{228}-*b*-PAI_{11}, initially at 1 wt% in a mixture of 5 wt% of DMF and 95 wt% of THF (5/95) trapped at various water contents.

Fig. 6 shows micrographs of morphologies obtained from a mixture of 5 wt% of DMF and 95 wt% of THF (5/95). At a water content of 17 wt% (Fig. 6A), which corresponds to 5 wt% of water above the cwc, spheres and compound micelles were seen. At higher water content, 25 wt% (Fig. 6B), the morphology changed to indented structures, which can be somehow related to the bowl-shaped morphology. With a further increase in the water content, the morphology goes to vesicles coexisting with rods and finally to almost solely vesicles. The presence of only 5 wt% of DMF made possible the formation of vesicles at high water contents for the triblock PAI_{11}-*b*-PS_{228}-*b*-PAI_{11}, differently to what was found in pure THF—the bowl-shape (BS).

At a composition of 10 wt% of DMF, at a water content of 5 wt% above the cwc (Fig. 7A), compound micelles are seen, but with smaller average size (40 ± 15 nm) when compared to Fig. 6A (45 ± 17 nm). The higher content of DMF, decreased the aggregate sizes at the early stages of water addition and favored the formation of BS coexisting with primary micelles at 25 wt% of water and lamellae at 35 wt% of water. At 50 wt% of water, vesicles were formed, identically to what was observed in Fig. 6D, that is, at higher water contents, the increase of 5 wt% of DMF on the final solvent composition did not affected the final morphology (compare Figs. 6D and 7D).

Frequently, structures superficially resembling biological and cellular systems were found in some copolymer systems. Since the sizes are typically quite different from the biological structures and obviously only morphologically, and not functionally biomimetic, this analogy cannot be taken very far; therefore these aggregates were called pseudo-biomimetic, or morphologically biomimetic. As an

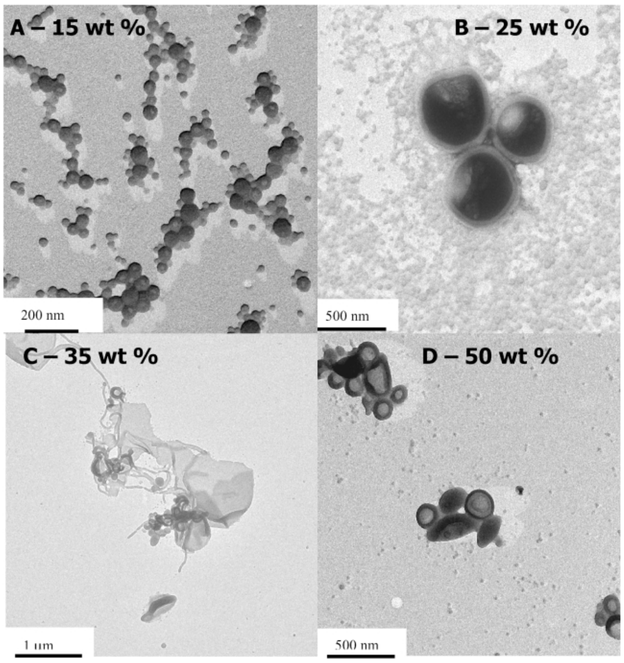

Fig. 7. TEM images of morphologies obtained from PAI_{11}-*b*-PS_{228}-*b*-PAI_{11}, initially at 1 wt% in a mixture of DMF and THF with 10 wt% of DMF (10/90), trapped at various water contents.

example we can cite the resemblance between the hollow bicontinuous tubular morphology with the smooth endoplasmic reticulum, among others [22]. An additional example of a biomimetic structure was found at the presently studied system, at 10 wt% of DMF and 35 wt% of water. Under these conditions, a morphology resembling dorsal root ganglia with extensive neurite outgrowth was identified (Fig. 8).

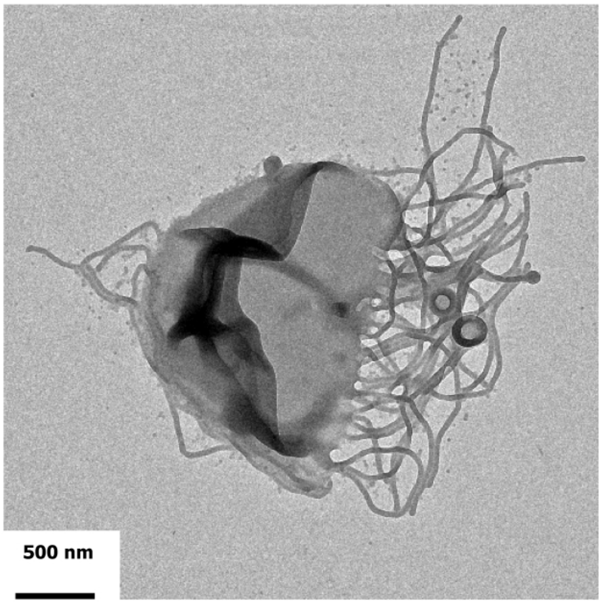

Fig. 8. TEM image of a pseudo-biomimetic morphology obtained from PAI_{11}-*b*-PS_{228}-*b*-PAI_{11}, initially at 1 wt% in a mixture of DMF and THF with 10 wt% of DMF (10/90), trapped at 35 wt% of water.

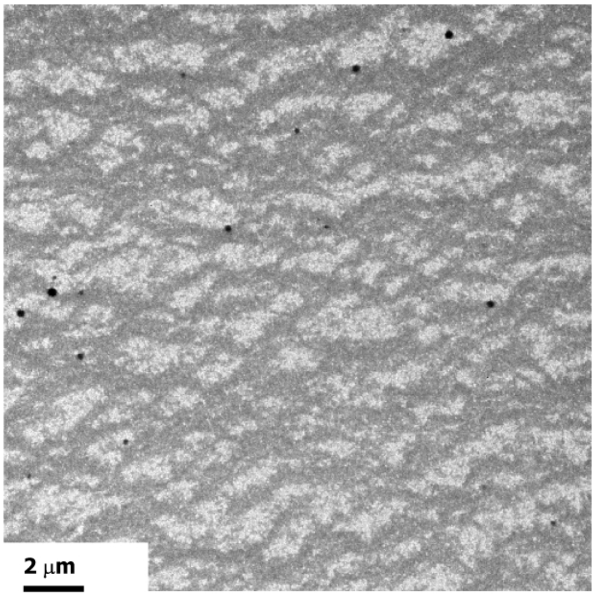

Fig. 9. Compound micelles and 2D micelle sheets. Solvent composition: 70 wt% of DMF.

When the DMF content is continuously increased, LCMs, bilayers and micelle sheets (Fig. 9) formation are favored. Two dimensional -2D- sheets of micelles were described as a near-equilibrium morphology [50], which might be precursor of lamellae.

3.4. Study of the stability of primary micelles

Light scattering techniques have been proven to be a valuable tool on the characterization of polymer micelles of various types [9,10,47,51,54]. Primary micelles were prepared by dissolving the copolymer PAI_{11}-*b*-PS_{228}-*b*-PAI_{11} in DMF at an initial concentration of 0.1 wt% (10^{-3} g/g) and then adding water as a precipitant, according to the procedure described in Section 2, followed by dialysis. The above condition of preparation lead to spherical aggregates with an average diameter of 23 ± 3 nm, as seen by TEM (Section 3.2). The PS core of these aggregates can be considered completely deswelled in aqueous solution.

After the dialysis step, the resulting colloidal solution concentration was 5.9×10^{-4} g/g (grams of copolymer per grams of solution). This so-called stock solution was then submitted to two sets of experiments. One consisted of adding DMF and the other adding water to the stock solution. The concentrations ranged from 5.9×10^{-4} to 5×10^{-5} g/g for the first set and from 5.9×10^{-4} to 8×10^{-6} g/g for the second set of experiments. The solutions were stirred overnight and let sit for at least 24 h before the laser light scattering experiments.

The intensity time correlation functions were obtained by photon correlation spectroscopy (DLS) for each individual solution. Relaxation rates, Γ, and apparent diffusion coefficients, $D_{app} = \Gamma/q^2$, were evaluated by CONTIN algorithm. The Stokes–Einstein equation, $D_{\mathrm{app}} = k_{\mathrm{B}}T/6\pi\eta_0 R_{\mathrm{h}}$, was used to evaluate the hydrodynamic radius, R_{h}, which constitutes a suitable approximation, since it can be assumed that only spherical aggregates are present in the stock solution, as evidenced by direct observation.

As a matter of convenience, the stock solution was considered to be composed of 100 wt% of water. Upon dilution with DMF, as done for the preparation of the first set of experiments, the solvent composition had to be recalculated for each solution. As a consequence, the refractive index, n, and the viscosity, η, were also determined for each solution as a function of the solvent composition.

The calculated values of $R_{\mathrm{h,app}}$ for the first set of experiments are summarized in Table 3. It is noteworthy that the $R_{\mathrm{h,app}}$ of the structures present on the stock solution (primary micelles in 100 wt% water) resulted 13.3 nm, which is within a very good approximation with the average radius determined by TEM (11 ± 2 nm). As DMF is added to the stock solution, the value of the $R_{\mathrm{h,app}}$ becomes gradually higher until the solution concentration drops to 2.0×10^{-3} g/g (34 wt% of water). Below this concentration, two values of $R_{\mathrm{h,app}}$ could be determined as a consequence of the bimodal distribution of the relaxation rates.

Typical examples of unimodal and bimodal non-weighted distributions of the relaxation rates given according to the CONTIN analysis, are showed in Fig. 10. At a concentration of 0.5×10^{-4} g/g, the first distribution lead to the calculus of a $R_{\mathrm{h,app}}$ of 116.9 nm and the second distribution to a $R_{\mathrm{h,app}}$ of 28.6 nm. Also, the contribution of the slow mode (centered at $\Gamma = 905\ \mathrm{s}^{-1}$), to the total amplitude is higher than the fast mode contribution (centered at $3697\ \mathrm{s}^{-1}$). Starting at 25.8 wt% of water (see Table 3), the slow mode contribution increases and the fast mode decreases as more DMF is added to the solution, and both $R_{\mathrm{h,app}}$ decreases with increasing dilution.

The above results may be explained by the following. Since DMF preferably solubilizes the PS rather than the PAI blocks, as DMF is added to a colloidal solution containing solely PAI-*b*-PS-*b*-PAI aggregates in water, the solvent molecules will be naturally driven towards the PS phase. Therefore, it is expected that the aggregate core will gradually become increasingly swollen as DMF is added to the solution. However, the ability of the whole structure to swell will be limited by the PS block length, i.e. there is a physical constrain to the unlimited stretching of the PS blocks. At a determined DMF content, due to the high degree of swollenness of the core, and the high degree of stretching of the PS chains, and also due to the environment polarity, it is no longer possible for the assembly of chains to exist as a micellar structure of the same type and with the same aggregation number than the original one. Additionally, because of the increased penalty for the decreased entropy of the core blocks, the stretching of the PS blocks cannot continue further. At this point, in order to decrease the total free energy, a very large inverse micelle forms in solution, which corresponds to the point where we first started detecting two relaxation modes. We believe that, the higher $R_{\mathrm{h,app}}$ accounts for the inverse micelle dimension and the lower one is ascribed to collective segment motions within the structure. In regard to the solvent composition effect, obviously, the interactions polymer/DMF and polymer/water play an important role on the stabilization of inverse micelle. This large aggregate is composed mainly by a PAI core with some trapped water molecules, and the outer layer is composed by the PS blocks surrounded by the DMF molecules. The formation of intermolecular aggregates, where the PAI blocks may belong to two different cores, being bridged by the PS blocks should also be considered. On continued dilutions, both $R_{\mathrm{h,app}}$ decreased with increasing DMF content, which is consistent to what we would expect, since as more DMF is added to the

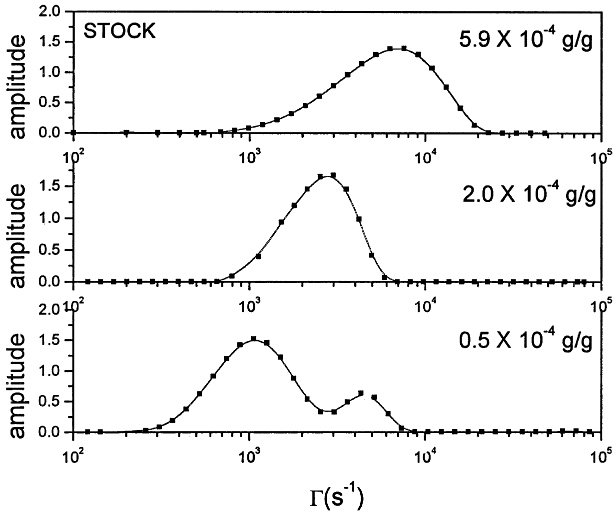

Fig. 10. Unimodal and bimodal distributions of the relaxation rates, given according to the CONTIN analysis. The solution concentrations are indicated.

Table 3
$R_{\mathrm{h,app}}$ obtained using the CONTIN algorithm for the solutions prepared upon dilution of the stock solution (5.9×10^{-4} g/g) with DMF. The scattering angle is $\theta = 90°$

Conc. (10^{-4} g/g)	5.9 (stock)	5.4	4.9	4.5	4.2	3.5	3.1	2.4	2.0	1.5	0.8	0.5
Water content (wt%)	100	91.6	83.3	76.6	71.6	60.0	52.9	40.8	34.2	25.8	15.0	9.2
$R_{\mathrm{h,app1}}$ (nm)	13.3	16.8	21.6	23.9	27.5	34.4	38.6	43.8	46.3	117	104	75.8
$R_{\mathrm{h,app2}}$ (nm)	–	–	–	–	–					28.6	20.7	19.0

solution, more water is extracted from the inside of the inverse micelle and as a parallel effect, the PS blocks would be better solvated. Relaxation rates obtained via CONTIN analysis are shown in Fig. 11.

On diluting the stock solution with water, the calculated $R_{h,app}$ did not change appreciably within the range of concentration. The stock solution constitutes a stable colloidal solution, where the primary micelles are already stabilized by water. So, as expected, the dilution of the micellar solution with water would not affect the resulting aggregates sizes.

3.5. Conclusions

A general investigation on the self-assembly behavior of di and triblock copolymers of styrene and quaternized 5-(*N*,*N*-diethylamino)isoprene in various solvents was carried out.

Starting as a homogeneous solution in either DMF, dioxane or THF, and adding water dropwise, the copolymers phase separate at a certain water content (cwc). The cwc was determined by SLS and it was found to be influenced by the nature of the organic solvent, and the copolymer initial concentration and architecture (di or triblock). The critical water concentration resulted higher in THF, lower in dioxane and lowest in DMF, and increased with decreasing copolymer concentration. The higher the initial concentration and the lower the degree of swollenness of the PS core in the final aggregate, the lower was the cwc.

The resulting aggregates from pure solvents and mixing solvents were investigated by TEM, under direct observation of the aggregates. A broad range of morphologies was found depending on the solvent, initial concentration and copolymer architecture. So far, spheres, rods, compound micelles and bowl-shaped structures were identified. The last one was already discussed in a recent publication.

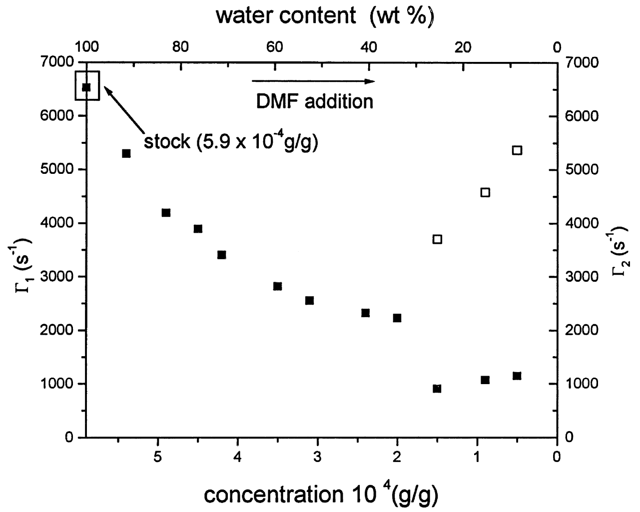

Fig. 11. Relaxation rates obtained via CONTIN analysis for the solution produced upon dilution of the stock solution with DMF.

Aggregates from the triblock PAI_{11}-*b*-PS_{228}-*b*-PAI_{11}, at an initial concentration of 1 wt%, were investigated employing mixtures of DMF and THF as the organic solvent. The studied morphogenic factors were the solvent composition and the content of water at which the solution was quenched. A much broader range of morphologies was found when comparing to pure solvents. These results confirm that the solvent effect is a useful tool on the morphological control of such aggregates.

Primary micelles from PAI_{11}-b-PS_{228}-*b*-PAI_{11} were prepared by first dissolving the copolymer in DMF at 0.1 wt%, and adding water to induce the aggregation. The solution was then dialyzed against deionized water to remove the organic solvent and to obtain a stable colloidal solution. The stability of such micelles was investigated upon dilution of the micellar solution with DMF and water, separately. The CONTIN algorithm was employed to calculate the hydrodynamic radius of the aggregates. Due to the higher affinity of DMF with the PS core, the dilution with this solvent causes the aggregates to swollen up to a point where it happens an inversion of the aggregates; and two modes of relaxation could be calculated in solution. The slow mode possible stands for the translational motion of the whole inverse micelle whereas the fast mode stands for collective segment motions within the aggregate. On the other hand, when water is used to dilute the colloidal solution, the apparent hydrodynamic radius did not change, as it was expected.

The newly investigated copolymer systems have shown multiple morphologies, i.e. aggregates with broadly adjustable properties can be obtained under specific preparative conditions.

References

[1] Astafieva I, Zhong X, Eisenberg A. Macromolecules 1993;26(26): 7339–52.
[2] Zhang L, Eisenberg A. Science 1995;268:721–7.
[3] Vinogradov SV, Bronich TK, Kabanov AV. Adv Drug Deliver Rev 2002;54(1):135–47.
[4] Bronich TK, Vinogradov SV, Kabanov AV. Nano Lett 2001;1(10): 535–40.
[5] Discher BM, Bermudez H, Hammer DA, Discher DE, Won YY, Bates FS. J Phys Chem B 2002;106(11):2848–54.
[6] Discher BM, Hammer DA, Bates FS, Discher DE. Curr Opin Colloid Interf Sci 2000;5(1–2):125–31.
[7] Breulmann M, Förster S, Antonietti M. Macromol Chem Phys 2000; 201:204–11.
[8] Landfester K, Rothe R, Antonietti M. Macromolecules 2002;35(5): 1658–62.
[9] Schuch H, Klinger J, Rossmanith P, Frenchen T, Gerst M, Feldthusen J, Müller AHE. Macromolecules 2000;33:1734–40.
[10] Loos K, Müller AHE. Biomacromolecules 2002;3(2):368–73.
[11] Jungmann N, Schmidt M, Maskos M. Macromolecules 2001;34(23): 8347–53.
[12] Maskos M, Harris JR. Macromol Rapid Commun 2001;22(4):271–3.
[13] Lu ZH, Liu GJ, Phillips H, Hill JM, Chang J, Kydd RA. Nano Lett 2001;1(12):683–7.

[14] Ding JF, Liu GJ, Yang ML. Polymer 1997;38:5497–501.
[15] Wang XS, Winnik MA, Manners I. Macromol Rapid Commun 2002; 23(3):210–3.
[16] Rosler A, Vandermeuler GWM, Klok HA. Adv Drug Deliv Rev 2001; 53(1):95–108.
[17] Allen C, Maysinger D, Eisenberg A. Colloids Surf B: Biointerf 1999; 16:3–27.
[18] Massey J, Power KN, Manners I, Winnik MA. J Am Chem Soc 1998; 120:9533–40.
[19] Moffitt M, Eisenberg A. Macromolecules 1997;30:4363–73.
[20] Gao Z, Varshey SK, Wong S, Eisenberg A. Macromolecules 1994;27: 7923–7.
[21] Tuzar Z, Kratochvil P, Matijievic E, editors. Surface and colloid science, vol. 15. New York: Plenum Press; 1993. p. 1.
[22] Cameron NS, Corbierre MK, Eisenberg A. Can J Chem 1999;77: 1311–26.
[23] Shen H, Eisenberg A. J Phys Chem 1999;103:9473–87.
[24] Zhang L, Eisenberg A. Macromolecules 1999;32:2239–49.
[25] Burke SE, Eisenberg A. Langmuir 2001;17:6705–14.
[26] Luo L, Eisenberg A. Langmuir 2001;17:6804–11.
[27] Shen H, Eisenberg A. Macromolecules 2000;33:2561–72.
[28] Yu Y, Zhang L, Eisenberg A. Macromolecules 1998;31:1144–54.
[29] Zhang L, Yu Y, Eisenberg A. Science 1996;272:1777–9.
[30] Burke SE, Eisenberg A. Langmuir 2001;17:8341–7.
[31] Châtellier X, Bottero JY, Le Petit J. Langmuir 2001;17:2782–90.
[32] Châtellier X, Bottero JY, Le Petit J. Langmuir 2001;17:2791–800.
[33] Fleer GJ, Cohen Stuart MA, Scheutjens JMHM, Cosgrove T, Vincent B. Polymer at interfaces. London: Chapman & Hall; 1993.
[34] Israelachvili J. Intermolecular and surface forces. London: Academic Press; 1992.
[35] Cameron NS, Eisenberg A, Brown R. Biomacromolecules 2002;3(1): 116–23.
[36] Cameron NS, Eisenberg A, Brown R. Biomacromolecules 2002;3(1): 124–32.
[37] Petzhold CL, Monteavaro LL, Stefens J. Polym Bull 2000;44:477–84.
[38] Petzhold CL, Morschhäuser R, Kolshorn H, Stadler R. Macromolecules 1994;27:3707–13.
[39] Petzhold CL, Stadler R. Macromol Chem Phys 1995;196:2625–36.
[40] Riegel IC, Samios D, Petzhold CL. Unpublished results.
[41] Bieringer R, Abetz V, Müller AHE, Stadler R. Eur Phys J 2001;5: 5–12.
[42] Burke SE, Eisenberg A. Polymer 2001;42:9111–20.
[43] Riegel IC, Petzhold CL, Samios D, Eisenberg A. In preparation.
[44] Riegel IC, Petzhold CL, Samios D, Eisenberg A. Langmuir 2002; 18(8):3358–63.
[45] Zhang L, Shen H, Eisenberg A. Macromolecules 1997;30:1001–11.
[46] Zhang L, Eisenberg A. Polym Adv Technol 1998;9:677–99.
[47] Föster S, Zisenis M, Wenz E, Antonietti M. J Chem Phys 1996; 104(24):9956–70.
[48] Shen H, Zhang L, Eisenberg A. J Phys Chem B 1997;101:4697–708.
[49] Zhang L, Barlow RJ, Eisenberg A. Macromolecules 1995;28: 6055–66.
[50] Zhang L, Eisenberg A. J Am Chem Soc 1996;118:3168–81.
[51] Yu G, Krummow AA. Abstr. of Papers, 222nd ACS Nat. Meeting, Chicago, IL, USA; 26–30 August 2001.
[52] Safran SA, Pincus P, Andelman D. Science 1990;248:354–6.
[53] Esselink FJ, Dormidontiva E, Hadziioannou G. Macromolecules 1998;31:2925–32.
[54] Tuzar Z, Lochmann L, Janata M, Munk P. Int J Polym Anal Charact 2001;6:437–44.